



ELSEVIER

International Journal of Mass Spectrometry 178 (1998) 43–50



# A double focusing mass spectrometer for geochronology

John R. De Laeter\*, Allen K. Kennedy

*Department of Applied Physics, Curtin University of Technology, Perth 6001, Western Australia*

Received 6 August 1997; accepted 10 March 1998

## Abstract

The performance characteristics of a double focusing mass spectrometer designed specifically for geochronology are described. The sensitive high resolution ion micro probe (SHRIMP II) mass spectrometer is ideally suited for in-situ analysis of uranium and/or thorium-bearing minerals to provide geochronological information on micron-sized domains of the minerals. SHRIMP II simultaneously meets the requirements of high mass resolution and high ion transmission efficiency together with good abundance sensitivity. SHRIMP II's excellent spatial and mass resolution, coupled with its high sensitivity, has enabled zircon geochronology to be revolutionized. (Int J Mass Spectrom 178 (1998) 43–50) © 1998 Elsevier Science B.V.

## 1. Introduction

Geochronology—the dating of geological events by radioactive isotopes—was initiated when Nier [1] demonstrated that the isotopic composition of lead extracted from uranium and thorium-rich minerals varied significantly, depending on the chemical composition and age of the minerals. This allowed measurement of the age of the minerals provided the half-life of the parent nuclides ( $^{235}\text{U}$ ,  $^{238}\text{U}$ , and  $^{232}\text{Th}$ ) were known. Aldrich and Nier [2] demonstrated that  $^{40}\text{K}$  decays to both  $^{40}\text{Ca}$  and  $^{40}\text{Ar}$  thus providing the basis for two further methods for measuring geological age.

Nier [3,4] departed from accepted mass spectrometric practice by designing a single stage machine based on a  $60^\circ$  sector field magnet. This mass spectrometer not only reduced the weight and power consumption of the electromagnet, but enabled the ion

source and detector to be removed from the influence of the magnetic field. The relative simplicity of the Nier mass spectrometer compared to the large  $180^\circ$  spectrometers and double focusing mass spectrometers hitherto in use, enabled mass spectrometry to be accessible to a wide group of scientists rather than remain as a specialised instrument in physics.

The juxtaposition of the availability of this new type of mass spectrometer and the establishment of age determination techniques by the U and Th–Pb and K–Ar radioactive decay systems, precipitated the development of geochronology in the early 1950s.

At that time, gas source mass spectrometry possessed sufficient sensitivity to analyze lead as lead hexafluoride or as lead tetraethyl for U and Th–U dating, and the noble gas argon for K–Ar geochronology. An electron impact ion source produced ions with a limited spread in energy which could be accommodated by the single stage magnetic sector field mass spectrometer. Another chronological technique, based on the decay of  $^{87}\text{Rb}$  to  $^{87}\text{Sr}$ , was later developed. Solid source mass spectrometers that use a

\* Corresponding author.

Dedicated to the memory of Al Nier.

thermal ionization source were able to analyze the isotopic composition of strontium isotopes extracted from whole rock samples to be measured with adequate sensitivity. Again, the energy spread of the ions was sufficiently small to enable the Nier-type mass spectrometer to be successfully used. As other geochronological techniques were established, such as  $^{176}\text{Lu}$ – $^{176}\text{Hf}$  and  $^{187}\text{Re}$ – $^{187}\text{Os}$ , the question of sensitivity became of increasing concern, and methods of enhancing the ionization efficiency of the thermal ion source were developed to overcome the limitations of sensitivity.

Another requirement of conventional geochronology was the necessity for extracting solid daughter products with sufficient purity to avoid “poisoning” the thermal ionization process. Thus chemical extraction techniques, usually involving ion exchange resins, were used to isolate the elements in question from the rock or mineral specimen. Thus, bulk samples were dated, although more recently, as the technology of geochronology has improved, zircon crystals have been analyzed for U and Th–Pb dating by conventional thermal ionization mass spectrometry [5].

Kober [6] showed that the analysis of single zircon crystals in a mass spectrometer ion source enabled discordant Pb to be evaporated under low temperature conditions whilst the concordant fraction was emitted at higher temperatures. This was an important advance in our understanding of the sometimes complex nature of zircons, and complemented the work of Krogh [7] who had demonstrated that one could improve the concordance of zircons by removing the surface of the crystals by abrasion.

An alternative approach in deciphering the geochronological history of zircons was by breaking up large crystals and analysing individual fragments [8]. Corfu [9] developed a system of breaking the tips off large zircon crystals in order to distinguish between more recent events compared to the age of crystallization of the zircon cores. These innovative techniques that used conventional mass spectrometry were not a complete answer to tackling the problems presented by zircon geochronology. An alternative approach is microanalysis, which can provide unique information about the timing, growth, and recrystal-

lization of U and/or Th bearing minerals, and hence help to decipher the origin of rocks and their subsequent geological history.

## 2. Double focusing mass spectrometry

The advantages of analyzing minerals in situ, without the need of chemical processing, together with an efficient ionizing source providing high sensitivity for all elements independent of ionization potential, are powerful incentives to geochronologists. Secondary ion mass spectrometry (SIMS) was applied to the determination of zircon ages by Hinton and Long [10], but a major problem was that interferences occurred in the mass region of Pb. Dr. W Compston, and his colleagues at the Research School of Earth Sciences at the Australian National University, realised that a double focusing ion microprobe mass spectrometer with high resolution would be required to resolve interfering isobars, and that this instrument would require energy focusing to compensate for the large energy spread of ions sputtered from the sample by a duoplasmatron ion source. In the early 1970's, an ion microprobe of high sensitivity and with a mass resolution  $M/\Delta M$  of at least 5000 (by using a  $\Delta M$  value measured at the 1% peak height) was not available, so the decision was made to build a sensitive high resolution ion micro probe mass spectrometer based on the design of Matsuda [11]. Details of the design and fabrication of the instrument are described by Compston [12].

Double focusing mass spectrometers have been successively refined since the early work of Aston [13]. These spectrometers were used to measure the atomic masses of the nuclides that led to the development of the binding energy curve. Extensive ion optical design to permit double focusing machines of ever-increasing resolving power to be constructed are described by De Laeter et al. [14]. In 1971 Matsuda and Matsuo [15] described a method for calculating the second order image aberrations of a double focusing mass spectrometer, and subsequently, Matsuda [11] showed it was possible to design such an instrument that attained complete second order focus-

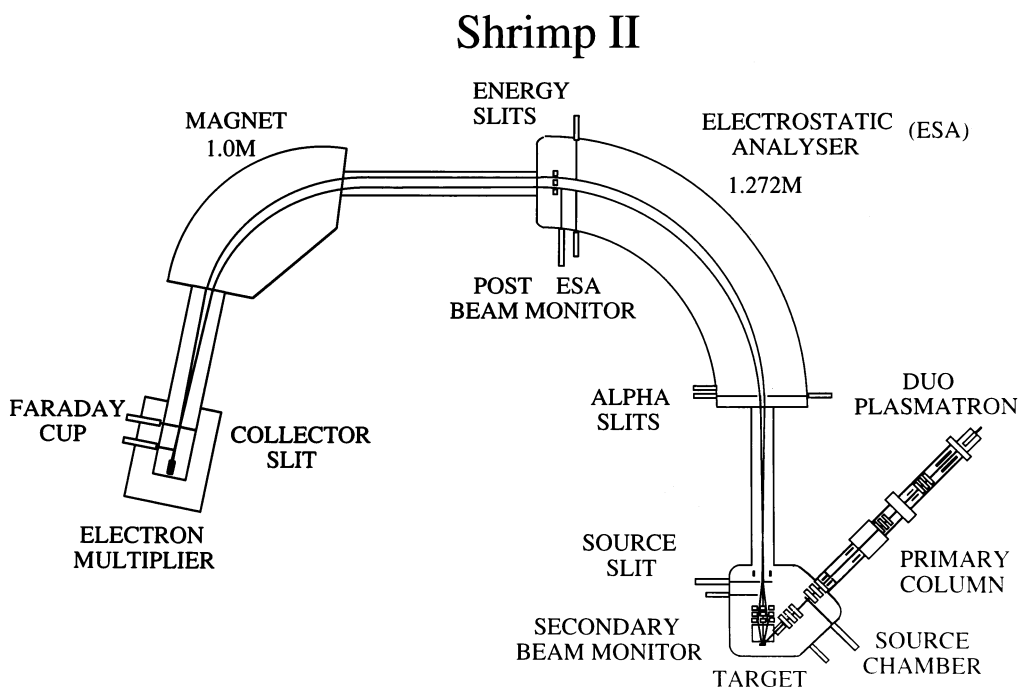


Fig. 1. Schematic of the SHRIMP II. The spectrometer comprises an  $85^\circ$  cylindrical electrostatic analyser of turning radius 1.27 m followed by a  $72.5^\circ$  sector magnet of turning radius 1 m.

ing. This instrument consisted of a cylindrical electrostatic analyser plus an electrostatic quadrupole lens, together with a homogeneous magnetic field. This configuration also possesses good vertical focusing characteristics. The design process included an examination of the influence of fringing fields with an accuracy effectively of third order. The Australian National University ion microprobe proved so successful for analysing zircon crystals in situ that a modified version (SHRIMP II) was constructed in the 1980s.

### 3. Performance characteristics of SHRIMP II

A consortium comprising Curtin University of Technology, the Geological Survey of Western Australia, and the University of Western Australia acquired a commercial version of SHRIMP II in 1993. After four years of operation it is appropriate that the performance characteristics of this mass spectrometer be described, together with an analysis of its limitations.

The configuration of SHRIMP II is shown schematically in Fig. 1. The production of secondary ions in SHRIMP II is achieved by ion impact sputtering. A primary beam of negatively charged ions is extracted from the oxygen plasma of a duoplasmatron ion source and accelerated to a potential of 10 kV. After focusing and steering, this beam is passed through a Wien magnet to produce a mass-filtered  $O_2^-$  beam that impacts at an angle of  $45^\circ$  onto the target. The primary beam size is defined by a circular aperture, the dimension of which can be selected as appropriate, and Köhler illumination provides a constant ion density. The image of the aperture is demagnified by a factor of six by using a pair of Einzel lenses, and the final result is a flat-bottomed,  $15 \times 25 \mu\text{m}$ , elliptical sputter crater, the size of which can be varied by altering the size of the aperture in the Köhler illumination section. The primary beam current is of magnitude 2 to 4 nA.

Samples are cast within a 24-mm-diameter, 5-mm-thick epoxy disk. The surface of the disk is ground

and polished flat so that the sample is exposed at approximately the midpoint section. A thin gold coat is applied to the mount by vapor deposition, producing a conductive surface that prevents charging during analysis. The sample manipulation system enables three samples to be stored in the vacuum lock together with two other samples in the specimen chamber. The surface of the target is cleaned prior to analysis by rastering of the primary beam for up to 5 min. This removes common lead on the sample surface.

Positively charged secondary ions are accelerated to 10 kV by the target being held at +10 kV relative to ground potential. The energy spread of the secondary ions is compensated for by an 85° cylindrical electrostatic analyzer (ESA) with a turning radius of 1.27 m, and a post-ESA quadrupole lens. Mass dispersion is achieved with a 72.5° sector magnet with a 1.0 m turning radius. The collector system consists of both a Faraday cup and electron multiplier that can be interchanged as required. A dead time of 32 ns has been measured for the electron multiplier and counting electronics.

The performance characteristics of the Perth Consortium SHRIMP II at a mass resolution  $M/\Delta M$  of 5000, by using a  $\Delta M$  value measured at the 1% peak height, are as follows:

- Mass discrimination: mass discrimination for  $^{208}\text{Pb}/^{206}\text{Pb}$  is respectively  $<0.5\%$  per amu for K feldspar (4% Pb);  $<0.3\%$  per amu for SRM610 glass (426 ppm Pb) and  $<0.1\%$  per amu for zircon (20 ppm Pb). For  $^{34}\text{S}/^{32}\text{S}$  in galenas the mass discrimination is approximately 3% per amu, being strongly dependent on the matrix being analyzed.
- Ion transmission: the ion transmission is calculated from a comparison of the number of ions emitted from an aluminum target to those collected at the Faraday cup in the collector assembly. The maximum transmission for  $\text{Ar}^+$  ions is 11%. Figure 2 illustrates that the transmission drops off rapidly as the resolution of the instrument is increased. At a mass resolution of 5000 the transmission efficiency is approximately 95% of the maximum possible. The transmission efficiency reduces to 17% of the maximum value

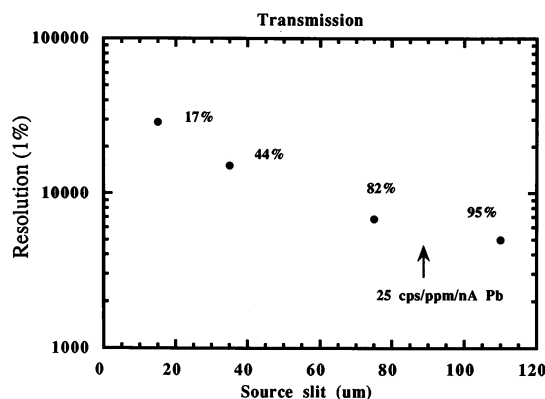


Fig. 2. The variation in the transmission of ions in SHRIMP II as a function of resolution is shown, together with the approximate values of the width of the source slit.

at a mass resolution of 30 000, which corresponds to a source slit width of approximately 15  $\mu\text{m}$ .

- Sensitivity: a sensitivity of approximately 20 CPS/ppm Pb/nA of  $\text{O}_2^-$  is achieved during routine U/Pb analysis of zircons.
- Abundance sensitivity: the abundance sensitivity is measured as the ratio of the background count rate at a fixed amu offset, divided by the count rate of the adjacent peak. Figure 3 shows the abundance sensitivity as a function of  $\Delta M$  (in amu) for uranium oxide and silicon. SHRIMP II is equipped with a retardation lens located in front of the collector, which enables the signals

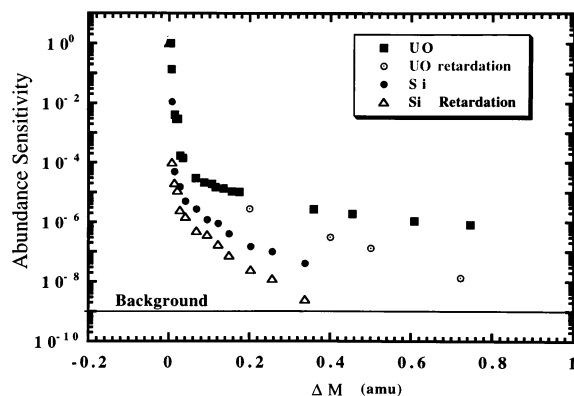


Fig. 3. The abundance sensitivity of SHRIMP II, with and without the retardation lens, is shown for  $^{238}\text{U}^{16}\text{O}^+$  and  $^{30}\text{Si}^+$ .

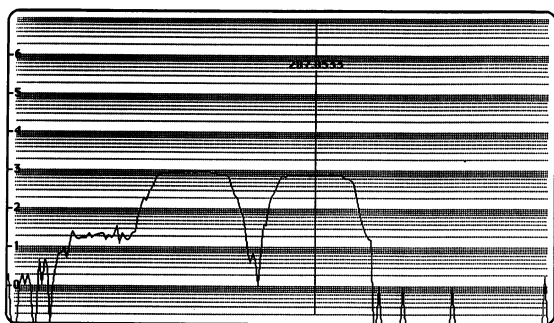


Fig. 4. The mass spectrum of  $^{176}\text{Hf}^{16}\text{O}_2^+$  and  $^{208}\text{Pb}^+$  (mass position 207.8533), at a resolution of approximately 5000, is shown for a standard zircon by using SHRIMP II. The vertical scale is logarithmic.

caused by the scattered ions to be reduced. The data displayed in Fig. 3 shows that the abundance sensitivity improves with the use of the retardation lens for both  $^{238}\text{UO}^+$  and  $^{30}\text{Si}^+$ . At 1 amu, the measured abundance sensitivity is  $6 \times 10^{-7}$  for  $^{238}\text{UO}^+$ , whereas with a retardation voltage of 10 014 V it is reduced to  $3 \times 10^{-8}$ . In the case of  $^{30}\text{Si}^+$ , the abundance sensitivity is  $5 \times 10^{-8}$  at 1 amu offset for  $^{30}\text{Si}^+$ , and this abundance sensitivity can be achieved at an offset of 0.5 amu with the retardation lens in use.

- (e) Mass resolution: at a resolution of approximately 5000, which is typically used for zircon geochronology, the  $^{176}\text{Hf}^{16}\text{O}_2^+$  peak is resolved from the  $^{208}\text{Pb}^+$  peak as shown in Fig. 4.

#### 4. Standards

In order to use SHRIMP II for geochronological purposes it is necessary to monitor biases and machine drift during the analysis by using a suitable reference material. In the case of zircon geochronology, gem quality zircons from Sri Lanka are used. Details of the standard zircon used in this laboratory are given by Pidgeon et al. [16]. Conventional thermal ionization mass spectrometry U/Pb isotopic data on this CZ3 zircon standard gives a uranium concentration of approximately 550 ppm and a concordant age of 564 Ma. The CZ3 standard is always mounted

together with zircon grains extracted from each sample. This enables determination of the Pb/U ratios of the sample by using comparative data analysis. A reproducibility of approximately 2% can be routinely achieved for  $^{206}\text{Pb}/^{238}\text{U}$  for 15 analyses of the standard zircon, the uncertainty being largely determined by the homogeneity of the standard.

The calculation of  $^{206}\text{Pb}$ – $^{238}\text{U}$  ages is based on the assumption that the bias of the measured  $^{206}\text{Pb}^+ / ^{238}\text{U}^+$  ratio relative to the true ratio can be described by the same power law relationship as that between  $^{206}\text{Pb}^+ / ^{238}\text{U}^+$  and  $\text{UO}^+ / \text{U}^+$  for both the standard and sample. The confirmation of the empirical power law relationship, with an exponent of two, is described in detail by Claoué-Long et al. [17]. The  $^{206}\text{Pb}$ – $^{238}\text{U}$  age derived from the analysis of an unknown zircon is based on analyses of the reference standard with a known value of  $^{206}\text{Pb}/^{238}\text{U}$ . The uncertainty of the age of the unknown zircon incorporates the uncertainty of the  $^{206}\text{Pb}^+ / ^{238}\text{U}^+$  ratio of the standard. Our analyses of the measured Pb/U and UO/U ratios determined on our CZ3 standard supports the Claoué-Long et al. [17] value of approximately two for the exponent in the power law relationship. Figure 5 shows two U/Pb calibration lines obtained from measurements of our zircon standard CZ3 on two different days, along with data from a population of igneous zircons extracted from an acid volcanic rock Sp (see the Appendix). The filled symbols are data collected in a single 24 h analytical session. Each point is a single 15 min analysis and the 1 sigma uncertainties for these individual measurements are typical of SHRIMP II data. The two standard data sets show that there is significant variation of both U/Pb and UO/U with changing analytical conditions, and this necessitates mounting the standard and unknowns together and interspersing the analysis of both throughout an analytical session. The concentrations of U, Th, and Pb in the sample zircon are calculated by using a similar approach to that used for the calculation of U/Pb ratios, with the unknown referenced to the standard with known U, Th, and Pb abundances [18].

A similar situation with respect to standards exists for other accessory minerals. SHRIMP II is a versatile machine in that numerous other U- and Th-bearing

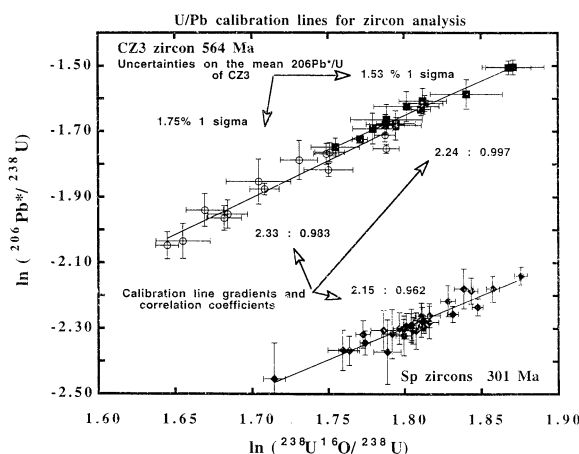


Fig. 5. U/Pb calibration lines for zircon analysis. Results from the Curtin zircon standard CZ3 on two days are shown, along with the results of measurements on a 301 Ma volcanic rock. The filled symbols for the standard and unknown are data from a single analytical session. The data for this plot are given in the Appendix. Uncertainties are 1 sigma and each point is a single 15 min analysis.

accessory minerals such as monazite, apatite, titanite, perovskite, rutile, and baddeleyite can be used for geochronological purposes. However, a problem in developing geochronological techniques for these minerals is in the availability of suitable homogeneous standards that must be characterised by conventional mass spectrometry and be present in sufficient quantity to overcome the difficulty of finding new standards from time to time. A review of the applications of SHRIMP II to various geochronological systems is given by Compston [12].

## 5. Limitations of SHRIMP II

After SHRIMP II was installed at Curtin University in 1993, it became apparent that there were severe vibration problems in the source region. This resulted from the cryopump being located immediately above the source chamber. The problem was solved by inserting a vibration-free isolation platform between the cryopump and the source chamber. Over the intervening period of time further refinements have been made so that vibrations have largely been eliminated in SHRIMP II.

The primary ion beam is generated by a hollow cathode duoplasmatron ion source designed especially for positive primary ion SIMS applications. It has the advantage of possessing dual polarity, but has the practical disadvantage of requiring maintenance on a regular basis. Our experience has been that approximately 60 days per year are required for maintenance and breakdowns on SHRIMP II, the largest component of this being in maintenance of the duoplasmatron ion source. Of more concern is the fact that when the duoplasmatron is reassembled its performance is not always reproducible, and it is difficult to reposition components in a manner that guarantees the desired performance. This appears to be a common problem with such ion sources.

The electromagnet that provides the high mass dispersion on SHRIMP II is controlled by multiple Hall effect probes. However, this large magnet inductance produces inherent time delay effects that necessitates leaving time between peak switching for the system to relocate in the center of the various mass peaks. In the case of U and Th–Pb geochronology, nine mass peaks are measured from mass number 196 ( $^{90}\text{Zr}_2\text{O}$ ) to mass number 254 ( $^{238}\text{UO}$ ). If a multicollector, capable of measuring all peaks simultaneously was available, it would result in an improvement of approximately a factor of two in throughput efficiency, and would also produce higher quality data. At this time, no multicollector exists for SHRIMP II, and therefore the throughput of samples and the quality of the data is limited to some extent. It is pleasing to note that the Australian National University group have designed and are presently constructing a multicollector for SHRIMP II.

## 6. Conclusions

The sensitive high resolution ion microprobe mass spectrometer has not only revolutionized geochronology, but has also enabled a number of other important scientific problems to be successfully addressed. This large, double focusing secondary ion mass spectrometer, specifically designed for in-situ analysis of geological samples, simultaneously meets the requirements of high resolution and high transmission

efficiency. In terms of high spatial and mass resolution coupled with high sensitivity, SHRIMP II allows the frontier of zircon geochronology to be located within individual grains [19].

The ability to focus a 20  $\mu\text{m}$  ion beam on a single crystal in situ and measure the isotopic characteristics of that “spot” before moving to another nearby location, can provide an understanding of geological processes on a near to micron scale. Crystals, such as zircons, with complex structures, can therefore be examined to reveal their geological history. SHRIMP II is also ideally suited for cosmochemical studies, particularly for studying isotopic anomalies in meteoritic minerals [20]. SHRIMP II has also been applied to “light” elements—for example, in situ analyses of sulphur-bearing minerals can be achieved as isotopic or elemental sulphur measurements on selected areas of the sample [21]. The ability of SHRIMP II to measure the diffusion profile of a number of elements simultaneously gives invaluable information on the effects of ionic charge, ionic radius, and melt structure on diffusion in melts [22]. SHRIMP II can also be

used in measuring the activation energy and the mechanism of diffusion in solid-state diffusion processes.

The performance characteristics discussed in this article have shown that in terms of ion transmission efficiency, sensitivity, abundance sensitivity, and mass resolution, SHRIMP II is a double focusing mass spectrometer of outstanding merit, particularly for in situ geochronological purposes. Microanalysis will undoubtedly continue to impact the field as more instruments of this type become available.

### Acknowledgements

The authors would like to thank our colleagues in the Perth SHRIMP II Consortium for their input to this article and to Dr. D. Nelson who commented on an earlier version of this article. The Australian Research Council provided much of the funds which enabled SHRIMP II to be purchased, and also provides grants for ongoing research on this instrument.

### 7. Appendix

	Labels	$\ln(^{206}\text{Pb}/^{238}\text{U})$	$\pm \ln(^{206}\text{Pb}/^{238}\text{U})$	$\ln(^{238}\text{U}^{16}\text{O}/^{238}\text{U})$	$\pm \ln(^{238}\text{U}^{16}\text{O}/^{238}\text{U})$
0	CZ3-1	-1.7690	0.032 297	1.7488	0.008 318 6
1	CZ3-2	-1.7644	0.029 099	1.7510	0.009 714 6
2	CZ3-3	-1.8180	0.019 827	1.7502	0.01 617 5
3	CZ3-4	-1.7881	0.059 618	1.7309	0.01 221 4
4	CZ3-4b	-1.9525	0.043 176	1.6841	0.01 292 1
5	CZ3-5	-1.9642	0.037 278	1.6819	0.01 123 1
6	CD3-6	-1.8766	0.017 366	1.7083	0.01 761 4
7	CZ3-6b	-2.0346	0.053 839	1.6551	0.01 761 4
8	CZ3-7	-1.7118	0.020 229	1.7875	0.006 839 3
9	CZ3-7b	-1.7534	0.013 996	1.7883	0.008 565 3
10	CZ3-8	-1.8536	0.068 274	1.7043	0.02 117 3
11	CZ3-8b	-2.0479	0.041 000	1.6449	0.007 516 8
12	CZ-9	-1.9401	0.050 058	1.6693	0.01 218 2
13					
14	cz3-1	-1.6159	0.025 038	1.8136	0.01 198 7
15	cz3-2	-1.7489	0.027 156	1.7547	0.01 594 1
16	cz3-3	-1.5063	0.021 108	1.8680	0.01 475 1
17	cz3-4	-1.6773	0.019 372	1.7948	0.01 282 7
18	cz3-5	-1.6827	0.044 738	1.7944	0.01 719 0
19	cz3-6	-1.5044	0.022 805	1.8711	0.02 008 3
20	cz3-7	-1.5877	0.044 836	1.8408	0.02 338 0
21	cz3-8	-1.6924	0.046 762	1.7794	0.01 307 6
22	cz3-9	-1.6251	0.046 195	1.8017	0.02 144 9
23	cz3-10	-1.6653	0.046 721	1.7884	0.02 366 3

(continued)

Appendix  
(continued)

	Labels	$\ln(^{206}\text{Pb}/^{238}\text{U})$	$\pm\ln(^{206}\text{Pb}/^{238}\text{U})$	$\ln(^{238}\text{U}^{16}\text{O}/^{238}\text{U})$	$\pm\ln(^{238}\text{U}^{16}\text{O}/^{238}\text{U})$
24	cz3-11	-1.6345	0.017 734	1.8112	0.006 403 2
25	cz3-12	-1.7252	0.0070 098	1.7710	0.004 934 8
26	cz3-13	-1.6086	0.039 705	1.8124	0.01 558 5
27	zc3-14	-1.6796	0.030 941	1.7878	0.01 256 7
28					
29	Sp-1	-2.1785	0.060 180	1.8388	0.006 122 1
30	Sp-2	-2.3065	0.055 335	1.8077	0.006 345 2
31	Sp-3	-2.3053	0.040 621	1.8056	0.005 587 0
32	Sp-3b	-2.3678	0.044 520	1.7635	0.006 843 1
33	Sp-4	-2.2345	0.025 990	1.8478	0.003 466 0
34	Sp-5	-2.2886	0.048 055	1.8046	0.005 465 8
35	Sp-6	-2.2977	0.043 949	1.8044	0.004 651 8
36	Sp-7	-2.2804	0.049 410	1.8162	0.006 268 7
37	Sp-8	-2.1399	0.026 952	1.8757	0.004 095 5
38	Sp-8b	-2.2558	0.024 724	1.8316	0.003 534 1
39	Sp-9	-2.3010	0.029 815	1.7994	0.002 603 1
40	Sp-10	-2.3165	0.074 733	1.7917	0.006 768 1
41	Sp-11	-2.3661	0.061 332	1.7592	0.009 683 8
42	Sp-12	-2.2737	0.051 522	1.8108	0.004 996 2
43	Sp-13	-2.2919	0.039 045	1.8013	0.004 363 8
44	Sp-14	-2.1792	0.039 319	1.8576	0.004 258 0
45	Sp-15	-2.4541	0.10 956	1.7144	0.007 153 2
46	Sp-16	-2.1851	0.038 980	1.8436	0.004 447 7
47	Sp-17	-2.3053	0.061 064	1.7861	0.008 163 9
48	Sp-18	-2.2944	0.018 911	1.8128	0.003 343 1
49	Sp-18b	-2.2601	0.036 228	1.8164	0.006 986 9
50	Sp-19	-2.2159	0.047 110	1.8286	0.004 892 0
51	Sp-20	-2.3178	0.041 619	1.7726	0.004 784 6
52	Sp-21	-2.2996	0.048 338	1.7965	0.003 973 9
53	Sp-22	-2.2688	0.034 578	1.8117	0.004 924 3
54	Sp-23	-2.2776	0.020 441	1.8123	0.003 949 5
55	Sp-24	-2.2612	0.038 522	1.8113	0.004 245 1
56	Sp-25	-2.3714	0.098 210	1.7886	0.008 999 1
57	Sp-26	-2.3439	0.036 917	1.7740	0.003 346 8
58	Sp-27	-2.3217	0.060 754	1.7995	0.005 156 0

## References

- [1] A.O. Nier, Phys. Rev. 55 (1939) 153.  
[2] L.T. Aldrich and A.O. Nier, Phys. Rev. 74 (1948) 876.  
[3] A.O. Nier, Rev. Sci. Instrum. 11 (1940) 212.  
[4] A.O. Nier, Rev. Sci. Instrum. 18 (1947) 398.  
[5] B. Kober, Contrib. Mineral. Petrol. 93 (1986) 482.  
[6] B. Kober, Contrib. Mineral. Petrol. 96 (1987) 63.  
[7] T.E. Krogh, Geochim. Cosmochim. Acta 46 (1982) 637.  
[8] U. Scharer, C.J. Allegre, Nature 295 (1982) 585.  
[9] F. Corfu, Contrib. Mineral. Petrol. 98 (1988) 312.  
[10] R.W. Hinton, J.V. Long, Earth Planet. Sci. Lett. 45 (1979) 309.  
[11] H. Matsuda, Int. J. Mass Spectrom. Ion Phys. 14 (1974) 219.  
[12] W. Compston, J. R. Soc. West. Aust. 79 (1996) 109.  
[13] F.W. Aston, Philos. Mag. 38 (1919) 707.  
[14] J.R. De Laeter, P. De Bièvre, H.S. Peiser, Mass Spectrom. Rev. 11 (1992) 193.  
[15] H. Matsuda, T. Matsuo, Int. J. Mass Spectrom. Ion Phys. 6 (1971) 385.  
[16] R.T. Pidgeon, D. Furfaro, A.K. Kennedy, A.A. Nemchin, W. Van Bronswijk, U.S. Geol. Survey Circular 1107 (1994) 251.  
[17] J.C. Claoué-Long, W. Compston, J. Roberts, M. Fanning, Time Scales and Global Stratigraphy Correlation, Special Publ. 54 (1995) 3.  
[18] W. Compston, I.S. Williams, C. Meyer, J. Geophys. Res. 89 (1984) B525.  
[19] R.T. Pidgeon, J. R. Soc. West. Aust. 79 (1996) 119.  
[20] T.R. Ireland, W. Compston, Nature 327 (1987) 689.  
[21] C.S. Eldridge, W. Compston, I.S. Williams, J.L. Walshe, Int. J. Mass Spectrom. Ion Processes 76 (1987) 65.  
[22] A.K. Kennedy, K. Harris, T. Falloon, EOS Trans. Am. Geophys. Union 77 (1996) F660.